CHAPTER V
PREPARATION OF ETHYLENE (VINYL ACETATE)-G-POLYLACTIDE BY CATALYTIC REACTIVE EXTRUSION IN AN INTERMESHING CO-ROTATING TWIN-SCREW EXTRUDER

5.1 Abstract

The modified EVA produced at 10 rpm from the previous chapter was brought to react with PLA via catalytic reactive extrusion in order to develop the processibility of PLA with various contents of tin (II) octoate ($Sn(Oct)_2$) catalyst i.e. 0.1, 0.3, and 0.5%wt, and at the screw rotating speeds of 30 and 40 rpm. The EVA-g-PLA produced from this reaction was studied in its thermal properties, morphology, and physical properties.

keywords : Reactive extrusion, Graft copolymerization, EVA-g-PLA

5.2 Introduction

A variety of packaging and medical products produced from biopolymers, such as polylactide (PLA), are benefit from biodegradability within 4–5 weeks by heat, humidity and microorganisms [1,2]; however, polylactide has some disadvantages such as rigidity, brittleness and low toughness. The poor properties could be overcome by copolymerization or blending with other polymers. Usually, blends of PLA lack of biocompatibility and biodegradability; therefore, the suitable method for modification is copolymerization with careful consideration to retain biodegradability. In this work, graft copolymerization of polylactide onto ethylene (vinyl acetate) or EVA by using catalytic reactive extrusion was selected due to the biocompatibility and elastic properties of EVA, which can enhance the flexibility of PLA [3]. Moreover, the product can also be used as a compatibilizer in polymer blends [4].

There are two key reactions involving in preparation of graft copolymer by reactive extrusion. One is grafting reaction; grafting in an extruder reactor involves reaction of a molten polymer with a monomer or mixture of monomers capable of forming grafts to the polymer backbone. The second one is interchain copolymer

formation, which can be defined as reaction of two (or more) homopolymers to form copolymer. In the majority of cases the process involves combination of reactive groups of one polymer with reactive groups on a second polymer to form a block or graft copolymer. The process is usually run simply by intensive mixing of a melt of the two polymers in the extruder. Compatibilization of two immiscible polymers may be obtained through the presence of a block or graft copolymer of the two homopolymers which, when present at the interface of the two immiscible phases, acts as an emulsifying agent and lowers interfacial tension. Block or graft copolymers are most economically formed by reactive extrusion to form covalent or, less commonly, ionic bonds [5].

This chapter studied the effect of catalyst contents in graft copolymerization of PLA onto the modified EVA chains by catalytic reactive extrusion process with the help of tin (II) octoate ($Sn(Oct)_2$) catalyst, and the modified EVA produced at 10 rpm from the previous chapter.

5.3 Experimental

Materials

Ethylene (vinyl acetate) grade MV1055 was supplied by TPI POLENE Public Co., Ltd. Polylactide (PLA) grade 2002D, NatureWork, was purchased from Fresh bag Co., Ltd. Tin (II)-2-ethylhexanoate and Irganox®1076 were purchased from SM Chemicals (Sigma Aldrich).

Preparation of EVA-g-PLA

The preparation of EVA-g-PLA was done by catalytic reactive extrusion process in the twin-screw extruder from LabTech with L/D ratio of 20:1 (40-cm length and 2-cm diameter) and 2 die exits (3-mm diameter). The experiment will be done as follow: A mixture of 200 g modified EVA and 300 g PLA (the EVA to PLA ratio 40:60) was mixed with $Sn(Oct)_2$ catalyst (0.1, 0.3 and 0.5%wt) and 0.5%wt of Irganox®1076 (antioxidant) before fed into the hopper. The barrel temperatures and screw rotating speeds were set as shown in Table 5.1. Throughput was melt mixed again with the same extruder and the same condition in order to obtain better mixing.

Then the throughput was dry in vacuum oven overnight at 60°C before characterizations. In order to investigate the suitable amount of catalyst and screw rotating speed, thermal properties, thermal stability, mechanical properties, and morphology of the throughput were examined.

Fabrication of thin sheet EVA-g-PLA

The thin sheets of EVA-g-PLA were prepared by compression molding machine. The EVA-g-PLA pellets were dried in oven before fabication. The compression molding was performed by using a Wabash V50H Press with PTFE mold, at 190°C for 10-minute preheating and 5-minute compression with 5 tons compression force, then cooled down to 40°C and thickness in the range of 0.1–0.3 mm.

Characterizations

The structure of EVA-g-PLA was confirmed by H^1NMR (AVANCE300) at frequency of 300 Hz in $CDCl_3$.

TG-DTA curves were collected on a Perkin-Elmer Pyris Diamond TG/DTA instrument. The sample was loaded on the platinum pan and heated from 30°C to 800°C at a heating rate of 10°C/min under N_2 flow.

DSC analysis were carried out using a METTLER TOLEDO DSC822 instrument. The sample was first heated from 30°C to 190°C and cooled down to -30°C at a rate of 10°C/min under a N_2 atmosphere with a flow rate of 25 ml/min. The sample was then reheated to 190°C at the same rate.

Scanning electron microscopy (SEM) was performed on Hitachi S-4800 Model. The samples were compressed into 3-mm-thickness sheets by compression moulding machine at 190°C, 10-minute preheating and 10-minute compression. Then the samples were cryogenic fractured in liquid nitrogen, in order to prevent mobility of polymer chains, and were coated by platinum (Pt) to make them electrically conductive.

Young's modulus, Tensile Strength, and elongation at break were measured according to ASTM D 882-91 using a Lloyd Mechanical Universal Testing Machine with a 500 N load cell, a 100.00 mm/min crosshead speed and a gauge length 50 mm.

Test sample was cut into rectangular shape with a size of 10 x 150 mm and thickness in the range of 0.1-0.3 mm.

Table 5.1 Processing Temperatures of EVA-g-PLA from hopper to die exit

Type	Processing Temperatures (°C)										Screw Speed (rpm)
	Z1	Z2	Z3	Z4	Z5	Z6	Z7	Z8	Z9	Die	
EVA:PLA (0.1, 0.3, and 0.5%wt)	140	150	160	165	165	165	165	165	165	160	30
EVA:PLA (0.1, 0.3, and 0.5%wt)	140	150	160	165	165	165	165	165	165	160	40

5.4 Results and Discussion

5.4.1 Chemical Analysis

NMR

The structure of EVA-g-PLA was confirmed by H^1NMR (AVANCE300). EVA-g-PLA throughputs were dissolved in $CDCl_3$ then characterized at frequency of 300 Hz. The spectrum is shown in Figure 5.1. The H^1NMR spectrum of the sample shows chemical shift at 5.18 ppm corresponding to methine proton of the modified EVA, which attached to ester group.

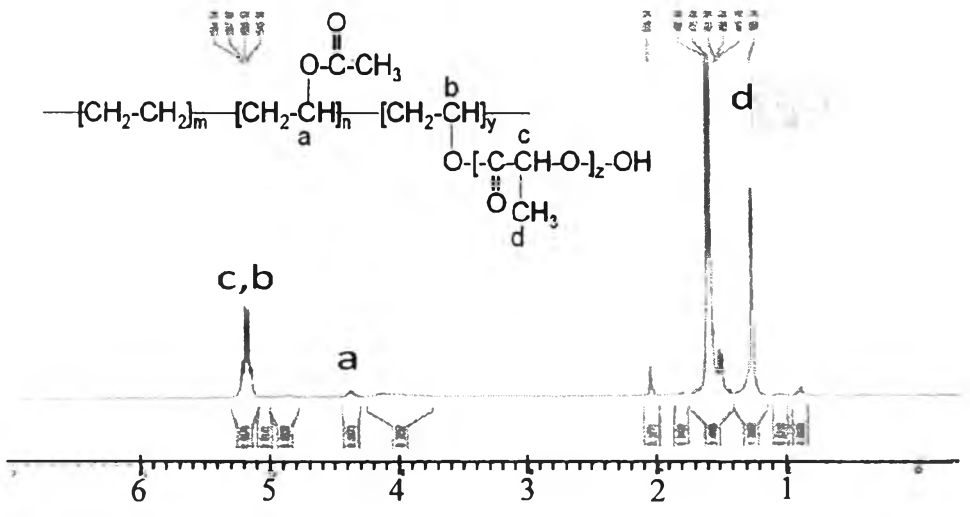

Figure 5.1 H^1NMR spectrum of EVA-g-PLA produced at 30 rpm with 0.3%wt $Sn(Oct)_2$.

5.4.2 Thermal Properties and Crystallization Behaviors

Decomposition temperatures, melting temperatures and crystallization temperatures of the EVA-g-PLA produced at 30 and 40 rpm with various catalyst contents are shown in Tables 5.2 and 5.3. The first released component, at temperature range of 240-260°C, was assigned to the PLA side chain, the second step, at temperature range of 310-330°C, was corresponding to acetate groups of modified EVA as well as homo-PLA, and the third component, at temperature range of 420-430°C, was ethylene backbone [7]. Figure 5.4 showed TGA thermogram of EVA-g-PLA produced at 30 rpm. Weight losses of the samples occurred in three steps, it also showed that the EVA-g-PLA contained 60%wt of PLA and 40%wt of EVA, which related to the beginning compositions. Moreover, the first degradation temperature of EVA-g-PLA, which was assigned to PLA side chain, was about 80°C lower than that of the commercial PLA. This can be assumed that the PLA side chain has lower molecular weight than the commercial PLA. The EVA-g-PLA produced at 40 rpm also shows three steps in weight losses as can be seen in Figure 5.5, but not equivalent to the beginning compositions, which was the evidence of non-homogeneous sample. Thermal stabilities of the copolymers produced at 30 and 40

rpm were lower than those of the pure EVA and pure PLA, due to the relatively low molecular weight fraction of the grafted chains [8].

Table 5.2 Decomposition temperature ranges of pure EVA and the modified EVAs at each screw speed

$Sn(Oct)_2$ (%wt)	Decomposition Temperature (°C)			Mass loss (%wt)		
	1st	2nd	3rd	1st	2nd	3rd
Pure EVA	-	310.7	429.5	77.8	-	21.4
Modified EVA	131.6	311.2	427.4	71.0	10.5	19.0
Pure PLA	-	332.5	-	-	-	99.8
EVA-g-PLA at 30 rpm						
0.1	258.1	328.6	428.7	31.6	59.9	8.3
0.3	249.8	321.1	428.5	22.6	62.2	7.8
0.5	244.6	317.5	430.3	28.6	63.0	8.1
EVA-g-PLA at 40 rpm						
0.1	258.3	320.7	431.8	53.6	30.5	14.7
0.3	241.7	316.9	429.2	29.3	62.1	8.6
0.5	248.7	321.6	430.7	48.7	37.6	13.3

DSC thermograms of EVA-g-PLA produced at 30 and 40 rpm are shown in Figures 5.6 and 5.7. All samples showed two distinct melting peaks, one attributable to the melting of PLA crystallites (from 120 to 140°C), another to ethylene crystallites (at about 70°C) [2]. These two melting peaks indicated the immiscibility of the samples [9]. Due to the conversion of graft copolymer was lower than those of the homopolymers [10]. T_m of the graft copolymer was lower than that of the neat PLA, as a result of complex structure and relatively low molecular weight of PLA side chains [4]. The crystallinity of the samples can be calculated from equation, where ΔH of standard sample was heat of fusion of perfect crystalline polymer; ΔH of perfect crystalline PLA is 93 J/g [11], and ΔH of perfect crystalline PE is 293 J/g [12].

$$\text{Crystallinity (\%)} = \frac{\Delta H \text{ of sample}}{\Delta H \text{ of standard sample}} \times 100$$

The EVA-g-PLA produced at 30 rpm present higher % crystallinity, as shown in Table 5.3. This is because higher screw speed (40 rpm) provided high shear force and temperature that can cause chain scission. The EVA-g-PLA produced at 30 rpm with 0.1 and 0.3%wt $Sn(Oct)_2$ showed the same %crystallinity of PE segment, which implied that the graft copolymer was produced at the similar amount. The EVA-g-PLA produced with 0.5%wt $Sn(Oct)_2$ has two separated crystallization temperatures resulting in more homopolymer produced from the reaction. The lower %crystallinity of PE segment also showed that PLA side chain can limit the crystallization of PE segment, and the %crystallinity of PLA segment also showed that homo-PLA was produced from the reaction more than the graft copolymer.

Table 5.3 Thermal Properties of EVA-g-PLA at 30 and 40 rpm with various catalyst contents (0.1, 0.3, and 0.5%wt)

$Sn(Oct)_2$ (%wt)	Decomposition Temperature			Melting Temperature				Crystallinity (%)		Crystallization Temperature	
	1st	2nd	3rd	1st peak	ΔH (J/g)	2nd peak	ΔH (J/g)	1st peak	2nd peak	Onset (°C)	Peak (°C)
Pure EVA	-	310.7	429.5	68.8	16.6	-	-	5.6	-	61.7	53.9
Modified EVA	131.6	311.2	427.4	69.8	14.3	125.6	0.4	4.9	0.2	117.2	52.9
Pure PLA	-	332.5	-	-	-	151.3	38.0	-	40.9	-	-
EVA-g-PLA at 30 rpm											
0.1	258.1	328.6	428.7	71.9	53.2	143.2	41.4	18.2	44.5	62.9	54.2
0.3	249.8	321.1	428.5	95.3	53.4	144.7	39.4	18.2	42.4	62.6	54.8
0.5	244.6	317.5	430.3	70.5	26.1	144.9	39.4	8.9	42.4	104.8, 62.2	94.2, 54.4
EVA-g-PLA at 40 rpm											
0.1	258.3	320.7	431.8	73.3	7.5	119.1	9.1	2.5	9.8	59.7	54.2
0.3	241.7	316.9	429.2	72.5	6.2	126.1	5.8	2.1	6.3	60.2	54.3
0.5	248.7	321.6	430.7	72.4	13.5	123.0	15.1	4.6	16.2	61.1	54.8

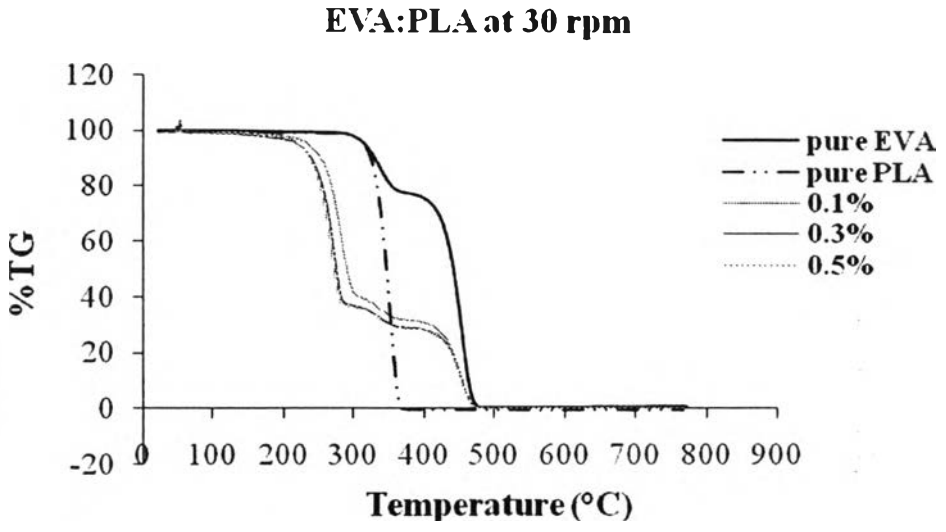

Figure 5.2 TGA plots of EVA-g-PLA (EVA:PLA, 40:60) at 30 rpm with various catalyst contents (0.1, 0.3, and 0.5%wt).

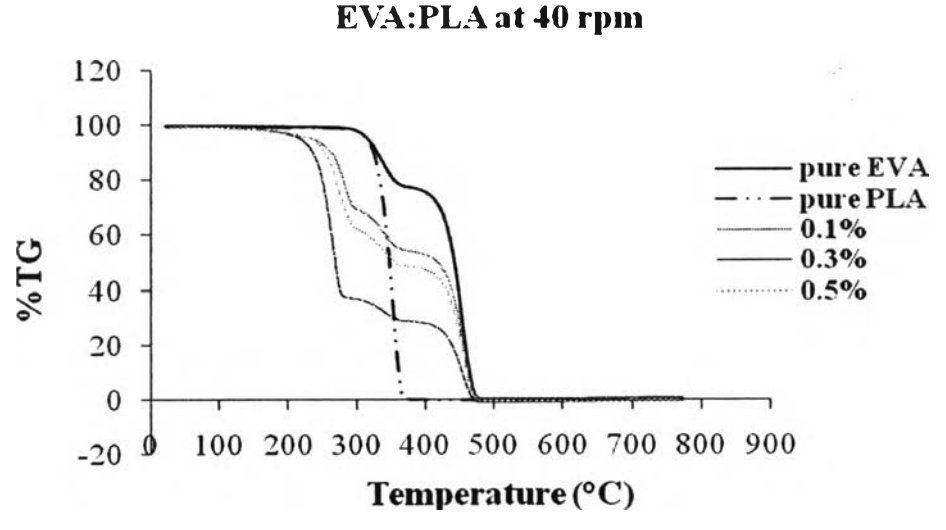

Figure 5.3 TGA plots of EVA-g-PLA (EVA:PLA, 40:60) at 40 rpm with various catalyst contents (0.1, 0.3, and 0.5%wt).

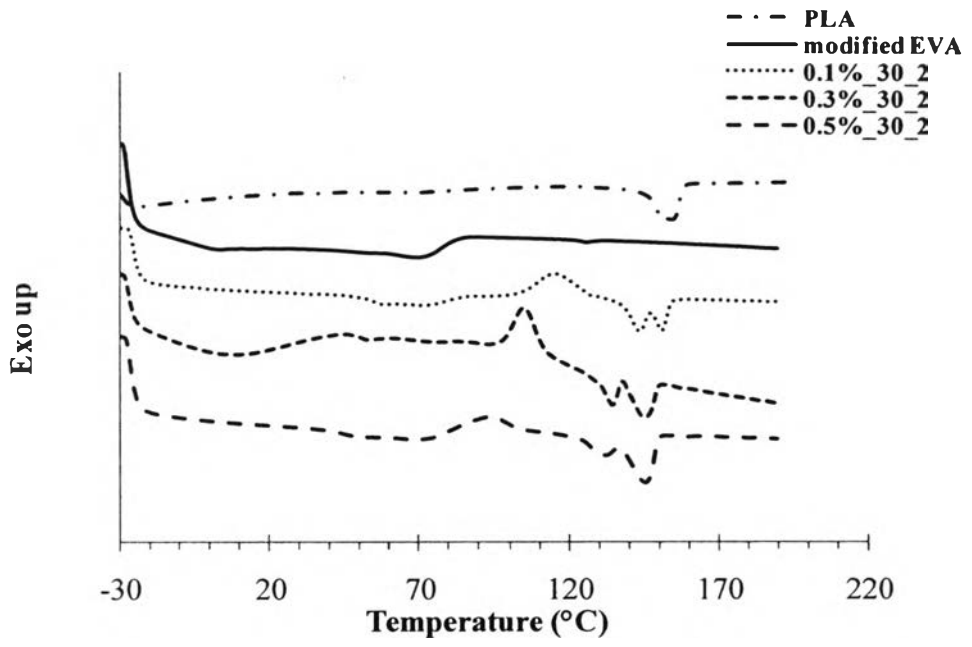

(a)

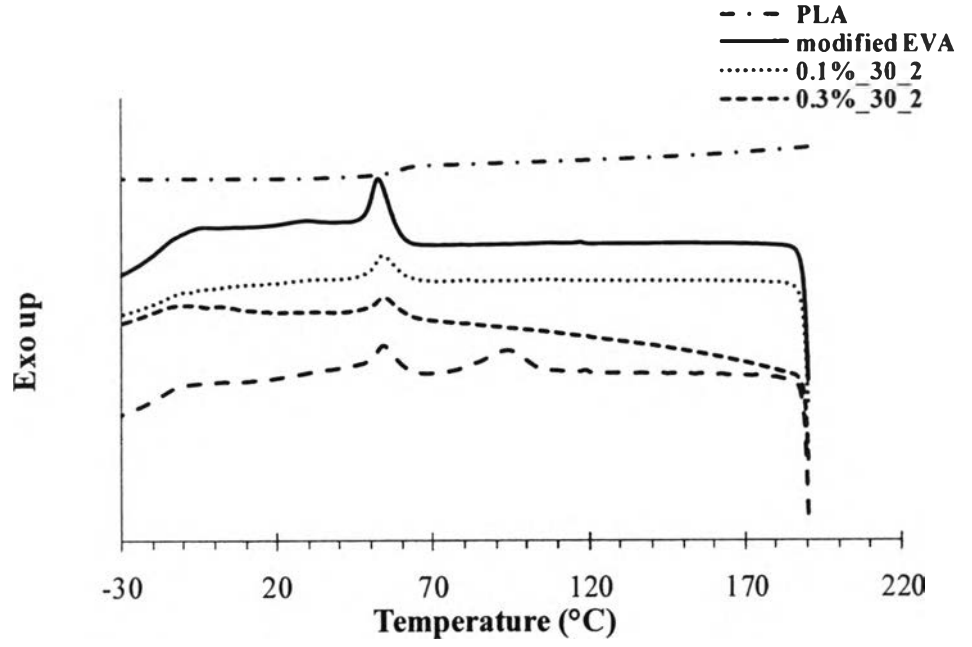

(b)

Figure 5.4 DSC thermograms of EVA-g-PLA (EVA:PLA, 60:40) at 30 rpm with various catalyst contents (0.1, 0.3, and 0.5%wt); (a) endotherm (2^{nd} heating), (b) exotherm.

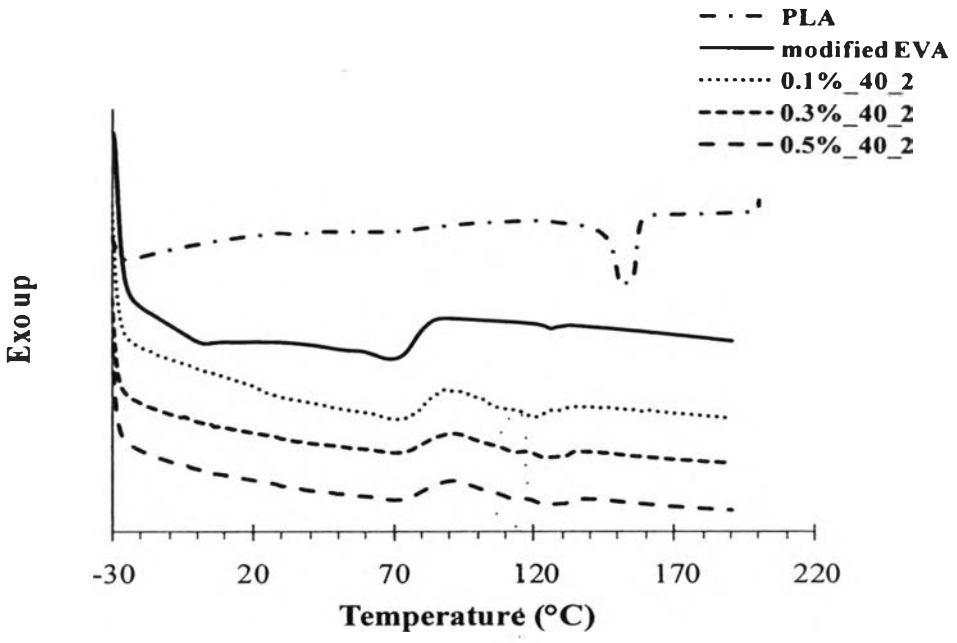

(a)

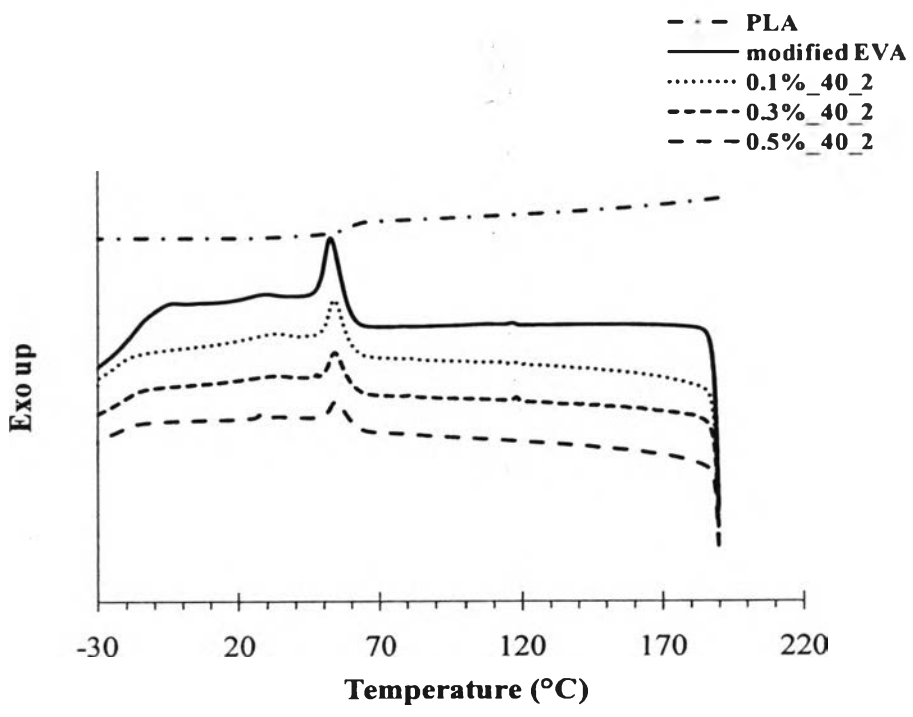

(b)

Figure 5.5 DSC thermograms of EVA-g-PLA (EVA:PLA, 60:40) at 40 rpm with various catalyst contents (0.1, 0.3, and 0.5%wt); (a) endotherm (2^{nd} heating), (b) exotherm.

5.4.3 Morphology

SEM

The morphology of samples were studied by SEM (Hitachi S-4800). SEM images of the EVA-g-PLA produced at various catalyst contents (0.1, 0.3, and 0.5%wt) and at screw speeds of 30 and 40 rpm are shown in Figures 5.8 and 5.9.

(a)

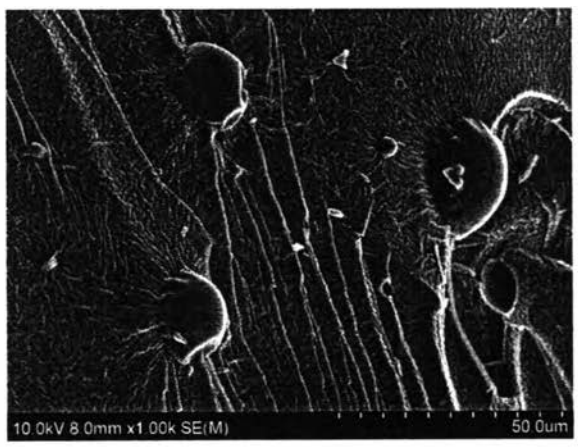

(b)

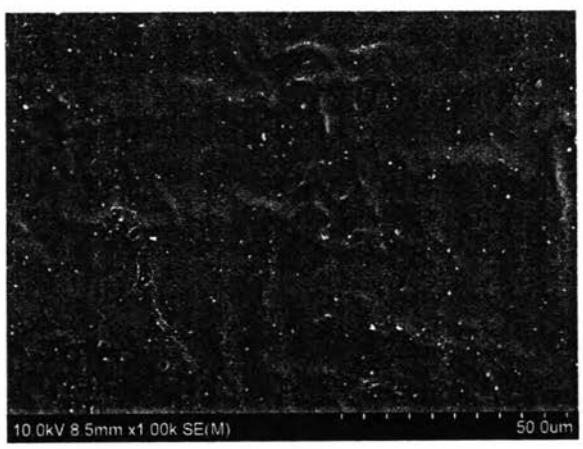

(c)

Figure 5.6 SEM images of EVA-g-PLA (EVA:PLA) at screw speed of 30 rpm and various catalyst contents; (a) 0.1%wt, (b) 0.3%wt, and (c) 0.5%wt.

(a)

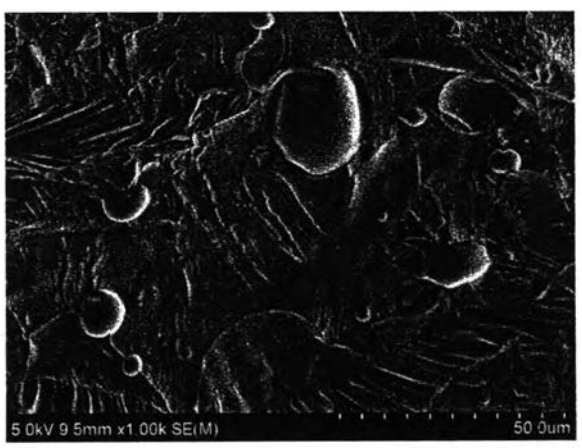

(b)

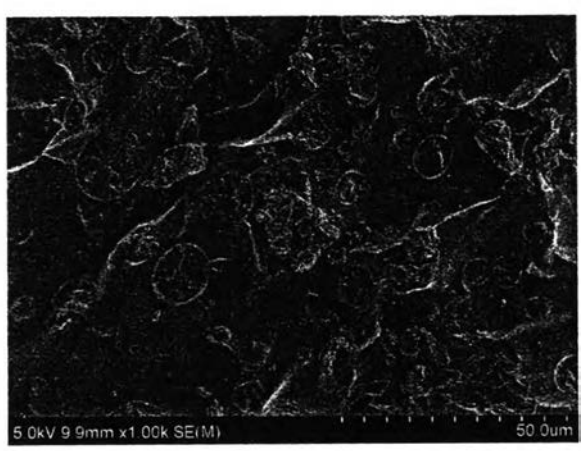

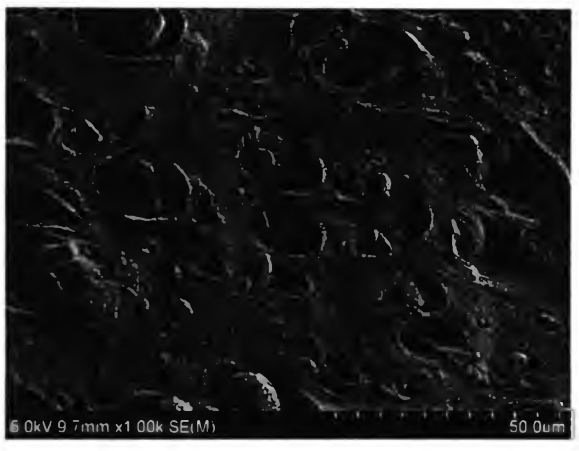

Figure 5.7 SEM images of EVA-g-PLA (EVA:PLA) at screw speed of 40 rpm and various catalyst contents; (a) 0.1%wt, (b) 0.3%wt, and (c) 0.5%wt.

Figure 5.8 and 5.9 indicated that phase separation was occurred for all catalyst contents (0.1, 0.3, and 0.5%wt), which suggested that the conversion of graft copolymer was lower than that of the homopolymer [9]. The phase separations are highly pronounced in EVA-g-PLA produced at 40 rpm (Figure 5.9), this might be a result of lower conversion of graft copolymer due to the higher screw speed [13].

Figure 5.8 (a) and Figure 5.9 (a) show that the catalyst content of 0.1%wt might not suitable for producing a desire amount of EVA-g-PLA, this caused phase separation to occur. Figure 5.8 (c) and Figure 5.9 (c) show that the catalyst content of 0.5%wt might be exceeded, which was subjected to homopolymerization of PLA [14]. Where the finest dispersion was found in EVA-g-PLA produced at 30 rpm with 0.3%wt catalyst (Figure 5.8 (b)), due to the effect of an interfacial interaction that caused by the formation of the graft copolymer [15].

5.4.2 Mechanical Properties

Tensile Properties Testing

Tensile Properties of EVA-g-PLA produced from various catalyst contents (0.1, 0.3 and 0.5%wt) at screw rotating speeds of 30 and 40 rpm were determined by Lloyd Mechanical Universal Testing Machine, according to ASTM D 882-91, with 500 N load cell, 100.00 mm/min crosshead speed and gauge length

of 50 mm. The specimens were prepared in a dimension of 10 mm × 150 mm (width × length) and thickness in range of 0.1-0.25 mm. The results are shown in Table 5.4.

Figure 5.10, EVA-g-PLA produced at 30 rpm with 0.1%wt $Sn(Oct)_2$ give the highest Young's modulus, where it presents the lowest % strain at break (Figure 5.12), due to the crystalline parts of the sample acts like hard segments resulting in chain stiffness, while tensile strength of the samples as shown in Figure 5.11are not much different. For EVA-g-PLA produced at 40 rpm, the sample with 0.1%wt $Sn(Oct)_2$ was too brittle to be examined. The sample with 0.3%wt $Sn(Oct)_2$ give higher Young's moduls than the sample with 0.5%wt, but it presents lower tensile strenght and % strain at break.

Table 5.4 The tensile testing results of EVA-g-PLA at various catalyst contetnts

Screw Speed (rpm)	Catalyst Content (%wt)	Young's Modulus (MPa)	Tensile Strength (MPa)	%Strain at Break
30	0.1	38.31(±16.2)	0.68(±0.09)	299.76(±58.7)
	0.3	28.98(±4.3)	1.12(±0.06)	498.74(±23.0)
	0.5	27.87(±8.9)	0.92(±0.10)	377.94(±46.01)
40	0.1	-	-	-
	0.3	36.17(±5.5)	0.10(±0.09)	448.88(±47.2)
	0.5	17.27(±1.6)	1.88(±0.09)	605.62(±34.6)
PLA		1817.66(±117.3)	10.88(±1.01)	5.20(±0.2)
Modified EVA		11.69(±0.5)	1.75(±0.08)	871.5(±26.6)

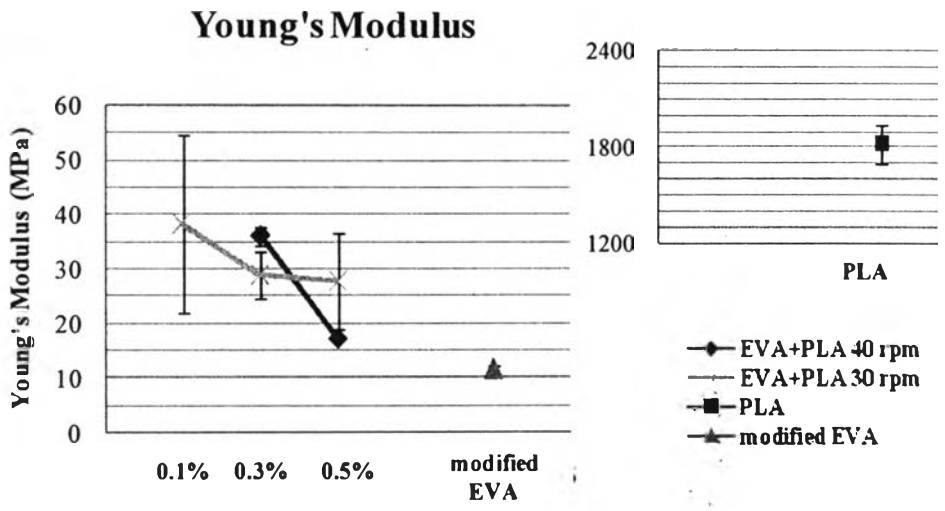

Figure 5.8 Young's modulus of EVA-g-PLA at various catalyst contents (0.1, 0.3, and 0.5%wt)

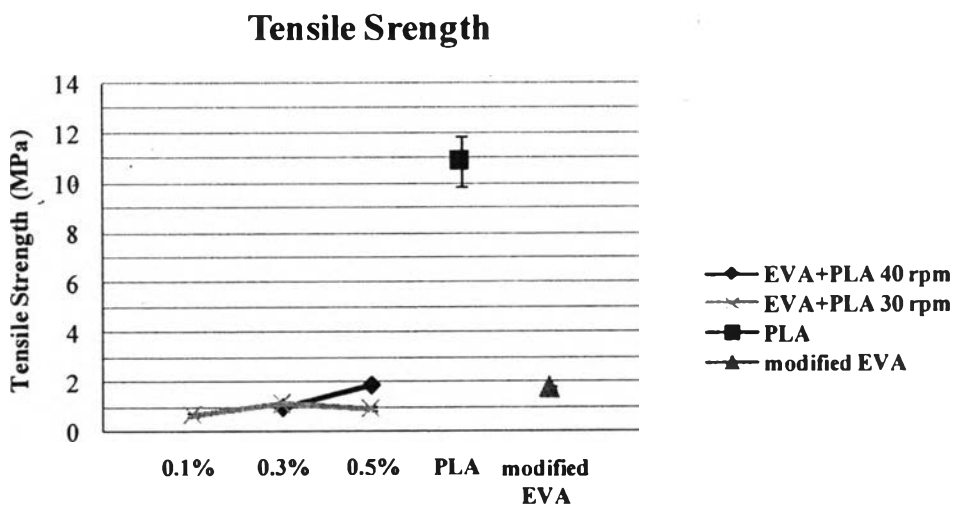

Figure 5.9 Tensile strength of of EVA-g-PLA at various catalyst contents (0.1, 0.3, and 0.5%wt)

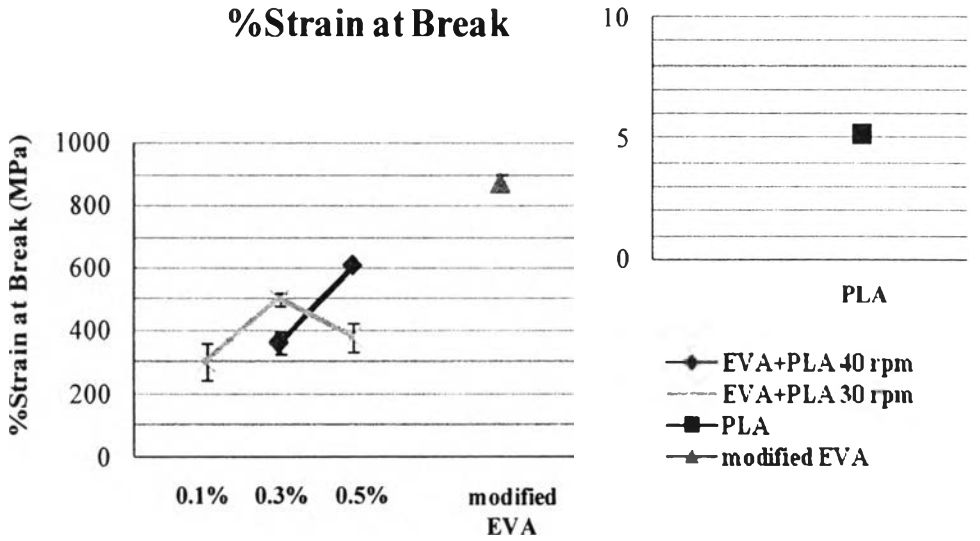

Figure 5.10 %Strain at break of EVA-g-PLA at various catalyst contents (0.1, 0.3, and 0.5%wt)

5.5 Conclusions

The EVA-g-PLA was synthesized by twin-screw extruder from LabTech with L/D ratio of 20:1 (40-cm length and 2-cm diameter) and 2 die exits (3-mm diameter) at various catalyst contents and srew speeds. The results from NMR and FTIR confirmed the existing of EVA-g-PLA. TGA-Thermogram of EVA-g-PLA produced at 30 rpm showed %weight loss corresponding to the original contents, where the graft copolymer produced at 40 rpm exhibited inhomogeneity. And the graft copolymer produced at 30 rpm exhibited higher crystallinity. Moreover, the SEM images of the graft copolymer produced at 30 rpm also showed better compatibility, where tensile properties were not much different from each other.Therefore, the suitable screw speed was 30 rpm and 0.3%wt was possibly be the suitable amount of catalyst giving the highest conversion of EVA-g-PLA with acceptable tensile properties, due to the finest dispersion.

5.6 Acknowledgements

This work is funded by the National Research Council of Thailand (NRCT), the Petroleum and Petrochemical College, and by the National Center of Excellence for Petroleum, Petrochemicals, and Advanced Materials, Thailand

I gratefully acknowledge the help of TPI POLENE.Co.Ltd, for the material support.

Finally, I would like to thank the help of Assoc. Prof. Rathanawan Magaraphan, Dr.Thanyalak Chaisuwan and Asst. Prof. Suparat Rukchonlatee for their suggestion of the experiment.

5.7 References

[1] Sudesh, K., Abe, H., and Doi, Y. (2000) Synthesis, structure and properties of polyhydroxyalkanoates: biological polyesters. Progress in Polymer Science, 25, 1503-1555.

[2] Ikada, Y., and Tsuji, H. (2000) Biodegradable Polyesters for Medical and Ecological Applications. Macromolecular Rapid Communications, 21, 117-132.

[3] Becquart, F., Taha, M., Zerroukhi, A., Kaczun, J., and Llauro, M.F. (2007) Microstructure and properties of poly(vinyl alcohol-co-vinyl acetate)-g-ε-caprolactone. European Polymer Journal, 43, 1549-1556.

[4] Jiang, H., He, J., Liu, J., and Yang, Y. (2002) Synthesis and characterization of poly(ethylene-co-vinyl alcohol)-graft-poly(epsilon-caprolactone). Polymer Journal, 34, 682-686.

[5] Brown, S.B. (1991) Annual Reviews of Material Science, 21, 409-35.

[6] Coates, J. (2000). Interpretation of Infrared Spectra, A Practical Approach. Chichester: John Wiley & Sons Ltd.

[7] Fernández, M.D., and Fernández, M.J. (2008) Thermal decomposition of copolymers from ethylene with some vinyl derivatives. Journal of Thermal Analysis and Calorimetry, 91(2), 447-454.

[8] Moraes, M. A. R., Moreira, A. C. F., Barbosa, R. V., and Soares, B. G. (1996) Graft Copolymer from Modified Ethylene–Vinyl Acetate (EVA) Copolymers. 3. Poly(EVA-*g*-Methyl Methacrylate) from Mercapto-Modified EVA. Macromolecules, 29, 416–422.

[9] Bhatia, A., Y., Rahul, K.G., Bhattacharya, S.N., and Choi, H.J. (2007) Compatibility of Biodegradable Poly(lactic acid) (PLA) and Poly(butylene succinate) (PBS) Blends for Packaging Application. Korea-Australia Rheology Journal, 19, 125-131.

[10] Hanley, S.J., Nesheiwat, A.M., Chen, R.T, Jamieson, M., Pearson, R.A., Sperling, L.H. (2000) Phase Separation in Semicrystalline Blends of Poly(phenylene sulfide) and Poly(ethylene terephthalate). II. Effect of Poly(phenylene sulfide) Homopolymer Solubilization of PPS-graft-PET Copolymer on Morphology and Crystallization Behavior. Journal of Polymer Science, 38, 4, 599-610.

[11] Xiao, H., Lu, W., Yeh, J.T. (2009) Crystallization behavior of fully biodegradable poly(lactic acid)/poly(butylene adipate-co-terephthalate) blends. Journal of Applied Polymer Science, 112, 6, 3754-3763.

[12] Salamone, J.C. (1996) Polymeric Materials Encyclopedia. USA: CRC Press, Inc.

[13] Zhu, W., Jaluria, Yo. (2004) Residence time and conversion in the extrusion of chemically reactive materials. Polymer Engineering and Science, 41, 1280-1291.

[14] Chen, L., Qiu, X., Deng, M., Hong, Z., Luo, R., Chen, X., and Jing, X. (2005) The starch grafted poly(L-lactide) and the physical properties of its blending composites. Polymer, 46, 5723-5729.

[15] Young, F.K., Chang, N.C., Young, D.K., Ki, Y.L., and Moo, S.L. (2004) Compatibilization of Immiscible Poly(l-lactide) and Low Density Polyethylene Blends. Fibers and Polymers, 5, 270-274.